

Simultaneous Cancellation of Beam Emittance and Energy Spread in the CEBAF Nuclear Physics Injector Chopping System *

H. Liu and J. Bisognano

CEBAF, 12000 Jefferson Ave., Newport News, VA 23606

Abstract

The CEBAF nuclear physics injector will utilize a unique chopping system consisting of two identical square box RF cavities with an inverting lens and a chopper aperture in-between. This system produces three interleaved 499 MHz cw electron beams from a 100 kV input beam. In this paper, we present our theoretical and numerical studies on how both emittance and energy spread are cancelled simultaneously in the dechopping process in the second cavity.

I. INTRODUCTION

The CEBAF nuclear physics injector chopping system consists of two identical square box RF cavities with a Newtonian lens and a chopper aperture in-between. The system produces three interleaved 499 MHz cw electron beams from a 100 kV input beam. In the first cavity, a beam is deflected radially and swept into a circle at the chopper aperture by two orthogonal electromagnetic modes (TM_{120} and TM_{210}) in the cavity. Each complete circle of the beam is chopped into three bunches continuously with three equally spaced notches at the chopper aperture. Then the bunches are brought back onto axis using the second cavity.

One interesting issue is whether the energy spread of electrons introduced in the first cavity due to finite beam spot size is cancelled or not as the beam is dechopped in the second cavity. In this paper, we present our theoretical and numerical studies.

II. LAYOUT OF THE SYSTEM

The layout of the initial part of the CEBAF nuclear physics injector is shown in Fig. 1. Following a 100-kV

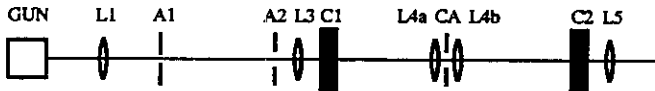


Fig. 1 Layout of the system

thermionic gun, a pair of apertures (A_1 and A_2) are used for limiting the emittance of the beam, which is 66 nm divided by the beam energy in MeV as the rms geometric emittance for the machine at high energies [1]. Then a pair of chopper cavities (C_1 and C_2) are used to chop a cw beam through an aperture (CA). The first lens (L_1) focuses the beam to a waist at the first aperture; the third lens (L_3) makes an image-to-image transform from A_1 to

CA ; and the lens pair L_{4a} - L_{4b} makes an image-to-image transform between the centers of C_1 and C_2 . The chopper system is symmetric with respect to the chopper aperture. The chopping process is shown in Fig. 2.

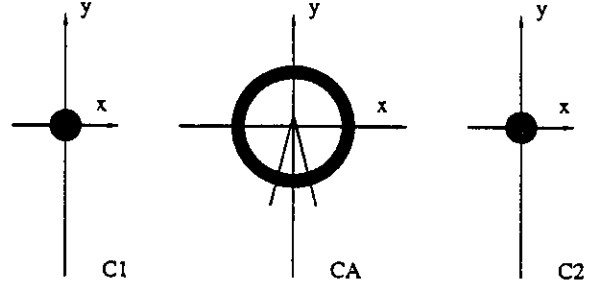


Fig. 2 Chopping process

III. CHOPPER CAVITY

Each chopper cavity is simply a square box operating at two orthogonal electromagnetic modes. Although the field distributions will be affected more or less by the beam pipe and coupling waveguide, the ideal field expressions for these two modes remain very useful and provide the most powerful means for us to get the most clear insight into the issue. We write these expressions as follows:

TM_{210} :

$$E_z = E_0 \sin(2\pi x/a) \cos(\pi y/a) \sin(\omega t), \quad (1.1)$$

$$B_x = -(\pi E_0/a\omega) \sin(2\pi x/a) \sin(\pi y/a) \cos(\omega t), \quad (1.2)$$

$$B_y = -(2\pi E_0/a\omega) \cos(2\pi x/a) \cos(\pi y/a) \cos(\omega t), \quad (1.3)$$

TM_{120} :

$$E_z = E_0 \sin(2\pi y/a) \cos(\pi x/a) \sin(\omega t), \quad (2.1)$$

$$B_y = (\pi E_0/a\omega) \sin(2\pi y/a) \sin(\pi x/a) \cos(\omega t), \quad (2.2)$$

$$B_x = (2\pi E_0/a\omega) \cos(2\pi y/a) \cos(\pi x/a) \cos(\omega t), \quad (2.3)$$

where a is the transverse dimension of the square box, and ω the angular RF frequency. The wavelength $\lambda=2a/\sqrt{5}$.

As can be seen from the above expressions, when its spot size is small, the beam centered on axis will experience a strong B_y field component from the TM_{210} mode and a strong B_x field component from the TM_{120} mode. When these two modes are excited in quadrature phase and equal amplitude, the electrons in an RF cycle will be swept into a circle in the transverse plane, and hence the longitudinal motion of the beam will be converted into transverse motion, providing an approach to chopping the

*Supported by D.O.E. contract #DE-AC05-84ER40150

beam into bunches in the transverse plane by using a number of notches. If the second cavity is added, the transverse momentum spread introduced in the first cavity can be compensated for from a reverse process. However, according to Eqs. (1.1) and (2.1), the finite beam spot size will introduce an additional energy spread as a side-effect. Will this energy spread be undone as the beam is dechopped in the second cavity? This is the issue we will study in this paper.

IV. INVERTING LENS

Before analyzing the performance of the chopping system, we introduce one crucial element in the system which is in fact an inverting lens consisting of two solenoidal lenses L_{4a} and L_{4b} .

Given that the system from C_1 to C_2 is symmetric with respect to the chopper aperture, the transfer matrix of the system is

$$R = \begin{pmatrix} R_{11} & R_{12} \\ R_{21} & R_{22} \end{pmatrix}$$

with

$$R_{11} = \left(1 - \frac{d_1}{f}\right)\left(1 - \frac{2d_2}{f}\right) - \frac{d_1}{f}, \quad (3.1)$$

$$R_{12} = 2\left(1 - \frac{d_1}{f}\right)\left(d_1 + d_2\left(1 - \frac{d_1}{f}\right)\right), \quad (3.2)$$

$$R_{21} = -2\left(1 - \frac{d_2}{f}\right)\frac{1}{f}, \quad (3.3)$$

$$R_{22} = R_{11}, \quad (3.4)$$

where d_1 is the distance from $C_{1(2)}$ to $L_{4a(b)}$, d_2 the distance from $L_{4a(b)}$ to the chopper aperture, f the focal length of the lenses. It is seen that for $d_1/f = 1$ and $d_2/f \ll 1$ the transfer matrix of the system becomes

$$R = \begin{pmatrix} -1 & 0 \\ -2/f & -1 \end{pmatrix}, \quad (4)$$

which describes a 180° flip to an electron. Since $f \gg d_2$, the crossover will take place between L_{4b} and C_2 .

The magnetic field of the solenoidal lens has been carefully measured[2]. We also calculated it using POISSON. Fig. 3 shows its field configuration from POISSON, and Fig. 4 shows the comparison of the on-axis field profile between the measurement and the calculation. The agreement in field profile is excellent. However, the calculated peak field actually was a few percent higher than the measurement. For example, for the same current of 0.9 A, the measured peak field is 153 Gauss, whereas the calculated one is 162 Gauss.

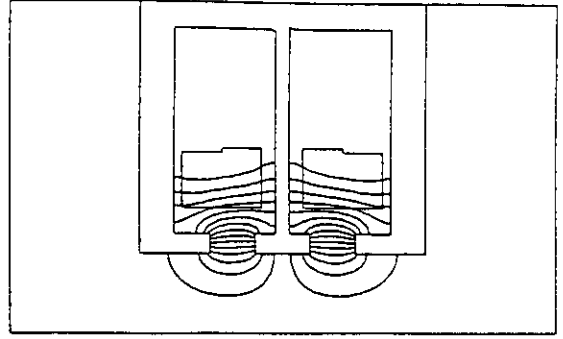


Fig. 3 Field configuration of the lens $L_{4a(b)}$ (POISSON)

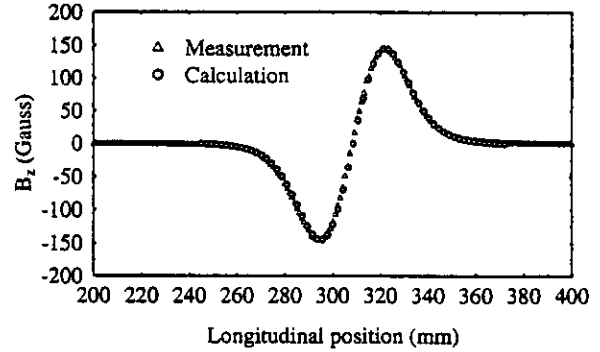


Fig. 4 Comparison of the field profiles for $L_{4a(b)}$

V. THEORETICAL ANALYSIS

The electromagnetic fields in a chopper cavity cause RF deflection and acceleration to electrons. From the TM_{210} mode, we have, to the first order of x and y ,

$$\Delta x' = -\theta_0[\sin(\phi) - \sin(\phi_{01})], \quad (5.1)$$

$$\Delta W_1 = W_0(x/a)[\cos(\phi) - \cos(\phi_{01})], \quad (5.2)$$

$$\Delta x = x'_0 \Delta z + a_0[\cos(\phi) - \cos(\phi_{01}) - \phi_x \sin(\phi_{01})], \quad (5.3)$$

where $\Delta x' = x'(t) - x'(t_0)$; $x' = v_x/v_z$ is the divergence angle; $x'_0 = x'(t_0)$; $\theta_0 = (|e|/m_0 c^2 \gamma)(E_0 \lambda / k a)$ is the deflection amplitude; $\phi = \omega t$ is the RF phase; $\phi_{01} = \omega t_0$ is the initial RF phase; $\gamma = 1/\sqrt{1 - \beta^2}$ is the relativistic factor; $\Delta W_1 = W_1(t) - W_1(t_0)$; $W_0 = |e|E_0 \lambda \beta_x$ is the energy spread amplitude; $\Delta x = x(t) - x(t_0)$; $a_0 = \theta_0 \beta_x / k$; $\beta_x = v_x/c$; $\phi_x = k \Delta z / \beta_x$; $\Delta z = z(t) - z(t_0)$; and all the other symbols have their conventional meanings.

Similarly, from the TM_{120} mode, we have

$$\Delta y' = -\theta_0[\sin(\phi) - \sin(\phi_{02})], \quad (6.1)$$

$$\Delta W_2 = W_0(y/a)[\cos(\phi) - \cos(\phi_{02})], \quad (6.2)$$

$$\Delta y = y'_0 \Delta z + a_0[\cos(\phi) - \cos(\phi_{02}) - \phi_x \sin(\phi_{02})], \quad (6.3)$$

where ϕ_{02} is the initial RF phase of the mode.

It is seen from Eqs. (5.2) and (6.2) that the maximum energy spread in a slice of a beam takes place from top to bottom or from right to left in the beam spot. So the

maximum energy spread for a slice of a beam, induced in a chopper cavity, is

$$\Delta W = m_0 c^2 \gamma k d \theta_0 \beta_z, \quad (7)$$

where d is the spot size diameter of the beam going through the cavity. Note that the maximum energy spread is proportional to the beam diameter. For the 1497 MHz chopping system, the slope is 100 eV/mm.

The maximum energy spread is related to the emittance in view of the fact that $\epsilon = d\theta_0/2$ is the beam emittance. Since the energy spread is induced due to the finite beam size, it must be a linear relationship between the emittance and the energy spread introduced, to the first order. This tells us that energy spread comes together with the emittance and therefore it is possible for it to vanish with the emittance as the latter is recovered in the second cavity.

In fact, there are two methods to recover the emittance and/or energy spread. One is to go through the same process that happened in chopper 1 reversely in chopper 2; the other is to go through the same process in the same direction in chopper 2 to make a closed course. It is pointed out that by the first method we can not recover the energy spread, since the energy spread is caused by the finite beam spot size and depends on electron trajectories, and the electrons can not suddenly move in the reverse direction because of the inertial effect. But we can recover both energy spread and emittance by the second method. Correspondingly, the first method requires that if the phase difference of the TM_{210} mode and the TM_{120} mode in the first chopper cavity is $+90^\circ$, it must be -90° in the second chopper cavity. For the second method it requires that the phase difference must be $+90^\circ$ in both chopper cavities.

VI. NUMERICAL MODELING

We used the code PARMELA for calculations. However, the conventional version of PARMELA assumes a hard-edge field profile for a solenoidal lens. It additionally requires that the length of the hard-edge field profile be the same as that of the rf element when the two elements overlap each other. The chopping process is treated using a zero-length transform. All these assumptions fail to apply to our case. We modified the code to meet the requirements for our modeling [3].

Numerically we easily found out that the phase difference between the two orthogonal modes must be $+90^\circ$ in both cavities, instead of $+90^\circ$ in one cavity and -90° in the other. This is consistent with the experiment. Then we found that the relative phase difference between the two identical modes in the two cavities governs the cancellation of emittance, and the energy spread follows exactly the same process as for the emittance, as shown in Fig. 5, given that the lenses L_{4a} and L_{4b} have been properly powered satisfying Eq. (4). The underlying mechanism is that an electron is flipped 180° in the transverse plane by

the inverting lens; and therefore it will experience an accelerating or decelerating process which is opposite to that which occurred in the first cavity.

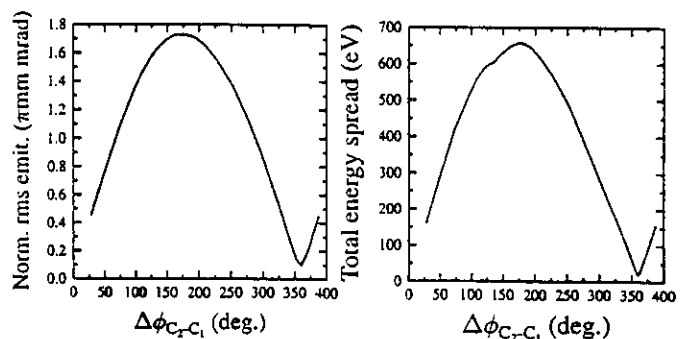


Fig. 5 Emittance and energy spread of the beam exiting the second chopper cavity versus the RF phase difference between the two identical modes in the two 1497 MHz cavities. The input bunch length in simulation is 360° , and 69° of it is chopped at the chopper aperture.

However, because of the finite transit angle, the cancellation both in emittance and energy spread could be incomplete. For example, for an RF cycle of electrons with an initial total energy spread of 10 eV and an initial normalized rms emittance of 0.08 mm mrad, the minimum energy spread and minimum normalized rms emittance at the exit of the second cavity in the 1497 MHz chopping system are 43 eV and 0.25 mm mrad, respectively, for the unchopped beam. However, for 69° of it chopped by the chopper aperture, the energy spread and normalized rms emittance are 23 eV and 0.11 mm mrad, respectively, as shown in Fig. 5. This issue will be further studied.

Some experiments carefully conducted by M. Tiefenback *et al.* will be presented in a separate paper [4].

VII. DISCUSSION

We believe this mechanism is not only important to our chopper performance but also of general interest. We point out that the extent of cancellation of the energy spread may depend on the coherence of the beam. The finite transit angle and any system aberrations will result in incomplete cancellation. In the future, we may do some more experiments on this issue as our commissioning schedule permits.

ACKNOWLEDGEMENTS

We thank C. K. Sinclair for various kinds of support and discussions. We also thank M. Tiefenback, G. Krafft and D. Douglas for discussions.

REFERENCES

1. H. Liu, CEBAF TN# 93-022.
2. C. K. Sinclair, private communication.
3. H. Liu, CEBAF PR-93-006.
4. M. Tiefenback and G. Krafft, this conference.